

Marc Seidel

Wave induced fatigue loads

Insights from frequency domain calculations

Offshore wind turbines are subject to dynamic excitation from wave loads. Especially when monopile substructures are used, significant fatigue loads can be induced by waves, which are then governing the design. Calculations in the frequency domain are very efficient to compute such wave induced loads and by applying some simplifications, very compact equations can be derived for the determination of fatigue loads. Such simplified formulas can be applied with good accuracy and important insight on governing parameters for wave induced fatigue loads can be gained. Based upon the formulas, further methods e.g. for lumping of scatter diagrams and for interpolations of fatigue loads for different positions within a wind farm can be derived.

Welleninduzierte Ermüdungslasten - Erkenntnisse aus Berechnungen im Frequenzraum. Offshore-Windenergieanlagen sind durch Wellen dynamisch angeregte Strukturen. Besonders bei Anlagen mit Monopile-Substruktur sind die welleninduzierten Ermüdungslasten oft dimensionierend. Berechnungen im Frequenzraum sind zur Berechnung von welleninduzierten Ermüdungslasten sehr effizient und mit einigen Vereinfachungen können sehr kompakte Formeln zur Ermittlung der Ermüdungslasten hergeleitet werden. Diese Formeln können mit guter Genauigkeit im Design-Prozess verwendet werden und die formelmäßigen Zusammenhänge erlauben wichtige Erkenntnisse bezüglich der Einflussparameter auf die Ermüdungslasten. Darauf basierend können weitere Methoden zur Kondensierung („Lumping“) von Seegängen oder zur Interpolation von Lasten zwischen individuellen Standorten innerhalb eines Offshore-Windparks entwickelt werden.

Keywords: Fatigue, Wave, Frequency domain, Lumping, Interpolation, Monopile

1 Introduction

As monopile substructures for offshore wind turbines (**Fig. 1**) gain market share in ever deeper waters [1], wave excitation becomes more and more important. It is therefore crucial to gain good understanding of the relevant parameters and to develop tools for rapid calculation of fatigue loads, which are typically governing for the structural dimensions. Calculations in the frequency domain are a helpful method in this respect and with some simplifications, which can be applied to offshore wind turbines supported by monopiles, very compact equations can be derived to compute wave induced fatigue loads.

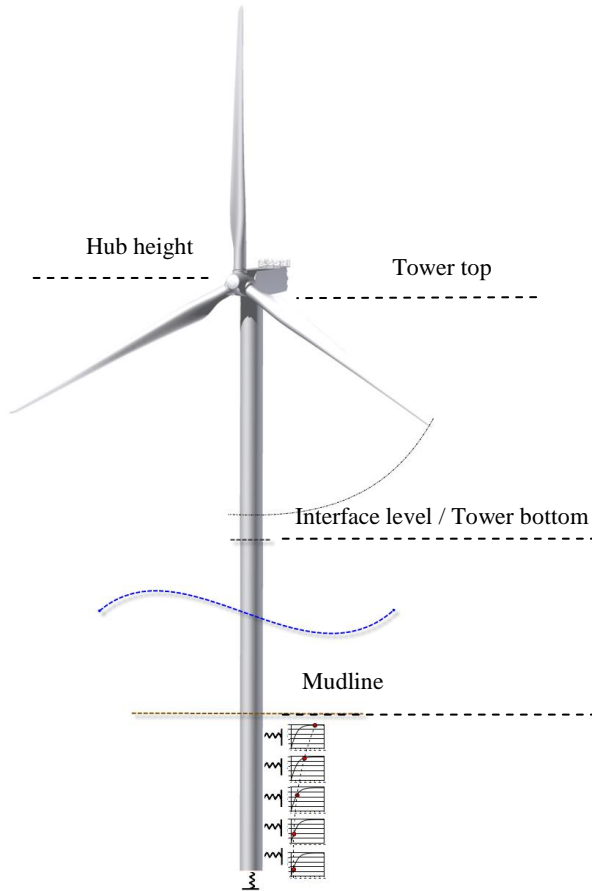


Fig. 1. Sketch of offshore wind turbine on monopile substructure

Abb. 1. Skizze einer Offshore-Windenergieanlage auf Monopile-Substruktur

2 Frequency domain analysis

Calculations in the frequency domain are a very powerful tool to compute wave induced response of offshore structures. General information about this method can be found in Hapel [2] and Barltrop [3]. Application to offshore wind turbines has been discussed (among others) by Kühn [4] and van der Tempel [5].

The general theory of frequency domain calculations is not repeated here for brevity. Symbols in general follow the notation used by Hapel [2], unless noted otherwise. In short, frequency domain calculations require the following calculations to be made:

1. Modal analysis is performed to determine natural frequencies ω_n and mode shapes $\Phi_n(z)$. Modal stiffness K_n and modal mass M_n are determined for each mode.
2. Modal damping ratios are assigned to the individual modes. In this particular case, only the modal damping ratio for the first mode is of importance. The damping is defined as damping ratio ξ (as a percentage of critical damping). Alternatively, this can be expressed with the logarithmic decrement δ , which relates to the damping ratio as $\delta=2\pi\cdot\xi$ for small damping ratios.
3. The wave spectrum $S_{\zeta\zeta}(\omega)$ is established for all sea states of relevance.
4. Transfer functions are determined:
 - a) The hydrodynamic transfer function $H_{a,n}(\omega)$ is needed to determine the generalized wave forces dependant on wave frequency ω and mode considered.
 - b) The mechanical transfer function $H_n(\omega)$ is needed to determine structural displacements dependant on the mode considered.

The combined transfer function is defined as:

$$H(z, \omega) = \sum_{n=1}^{\infty} \Phi_n(z) \cdot H_n(\omega) \cdot H_{a,n}(\omega) \quad (1)$$

Transfer functions can be generated to determine e.g. bending moments directly, rather than determining displacements first.

5. The response spectrum (e.g. displacements or bending moments at a specific elevation) is determined from the loading (wave) spectrum and the combined transfer function:

$$S_{uu}(z, \omega) = |H(z, \omega)|^2 \cdot S_{\zeta\zeta}(\omega) \\ = \left| \sum_{n=1}^{\infty} \Phi_n(z) \cdot H_n(\omega) \cdot H_{a,n}(\omega) \right|^2 \cdot S_{\zeta\zeta}(\omega) \quad (2)$$

6. Extreme or fatigue loads are determined from the response spectrum.

A typical example for the input spectrum (wave spectrum) and the corresponding response spectrum (spectrum of bending moment) is shown in **Fig. 2**. In the plot, the spectral quantities are plotted over frequency.

For this particular case, the following has been assumed:

- The structure is an offshore wind turbine founded on a monopile in 40m water depth, with a first natural frequency of $f_0=0.208\text{Hz}$, corresponding to a circular frequency $\omega=1.31$ 1/s.
- Damping ratio has been taken as $\xi_0=1\%$ of critical damping.
- The sea state is a typical fatigue sea state, with $H_S=2.0\text{m}$ and $T_p=6.0\text{s}$.
- The bending moment plotted is the moment at tower bottom (interface between tower and sub-structure), i.e. above the zone where direct wave loading is applied.

It can be seen that the response is narrow-banded around the first natural frequency $f_0=0.208\text{Hz}$, where significant dynamic amplification occurs.

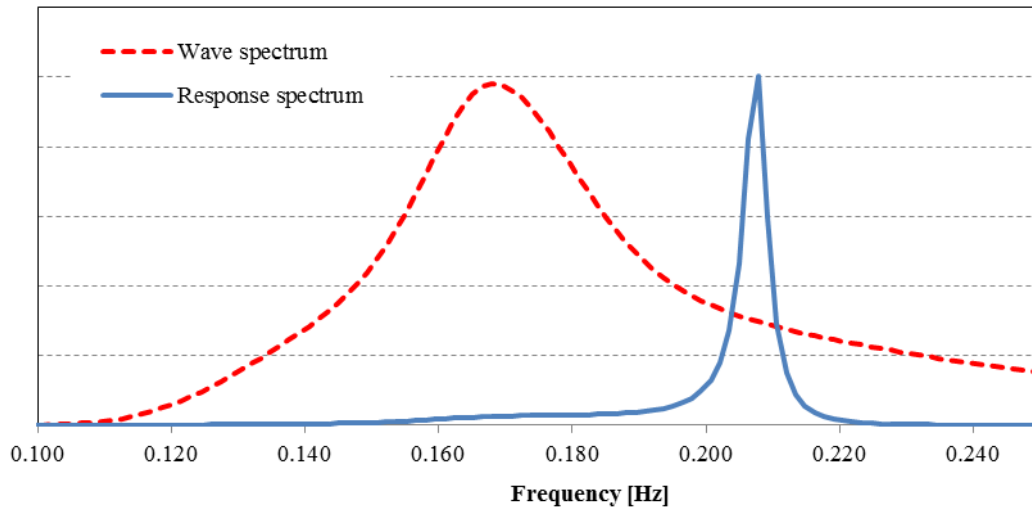


Fig. 2. Example for input (wave, dashed line) and response (bending moment at tower bottom, solid line) spectrum for $H_s=2.0\text{m}$, $T_p=6.0\text{s}$, $\xi=1.0\%$ (y-axes shown without values as figure just for illustration)

Abb. 2. Beispiel für Eingangs- und Antwortspektrum (Eingang Welle, Ausgang Biegemoment am Turmfuß) für $H_s=2.0\text{m}$, $T_p=6.0\text{s}$, $\xi=1.0\%$ (y-Achsen ohne Werte, da Diagramm nur zur Illustration)

In **Fig. 3** a second example is plotted, again for the same structure. This time, the plot is for a severe sea state with $H_s=8.0\text{m}$ and $T_p=10.0\text{s}$ and damping has been increased to 4% of critical damping for illustrative purposes. The response spectrum for the bending moment at seabed is now not a narrow-band spectrum, but has two peaks where the wave energy is highest and at first natural frequency.

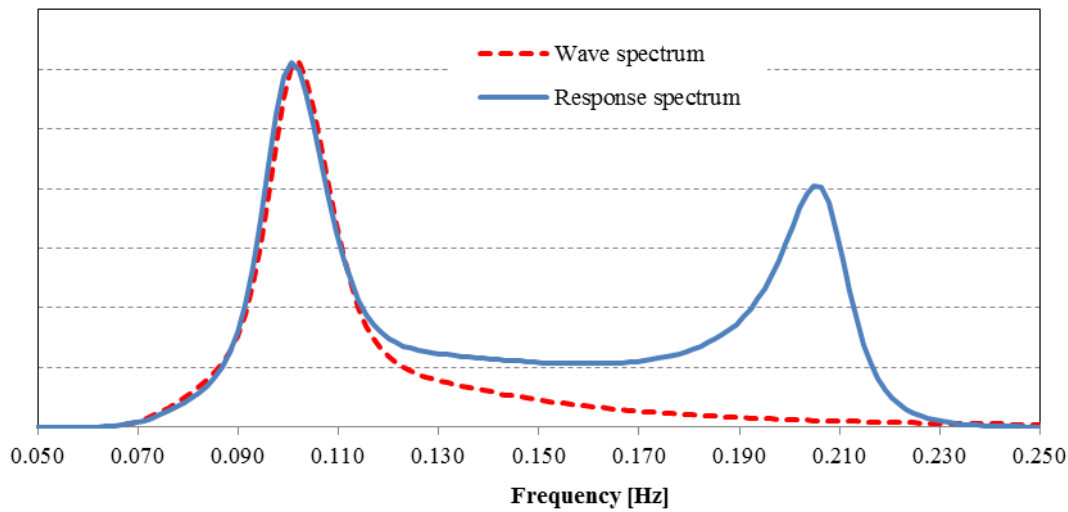


Fig. 3. Example for input (wave, dashed line) and response (bending moment at seabed, solid line) spectrum for $H_s=8.0\text{m}$, $T_p=10.0\text{s}$, $\xi=4.0\%$

Abb. 3. Beispiel für Eingangs- und Antwortspektrum (Eingang Welle, Ausgang Biegemoment am Seeboden) für $H_s=8.0\text{m}$, $T_p=10.0\text{s}$, $\xi=4.0\%$

Generally, the narrow-band assumption is a good approximation when damping is low. Damping ratios around 1% of critical damping are typically used for monopiles, therefore this assumption is valid.

3 A simplified method to determine wave induced fatigue loads

In this paper a simplified method to estimate wave induced fatigue loads on monopiles is presented. The required quantities and calculation steps are detailed in the following sections.

3.1 Wave spectrum

Short term sea states are typically represented by a wave spectrum, i.e. the power spectral density function of the sea elevation process, $S_{\zeta\zeta}(\omega)$. $S_{\zeta\zeta}(\omega)$ is a function of the significant wave height H_S and the peak period T_P and expresses how the energy of the sea elevation is distributed between various frequencies. Wave spectra for design purposes are given in the relevant codes and standards. The JONSWAP spectrum is often applied for North Sea conditions and is also used for the examples shown in this paper.

3.2 Assumptions for the proposed simplified method

The following simplifications are made, which are acceptable for offshore wind turbines mounted on monopile substructures:

1. Only the first mode is considered for response calculations, as higher modes are outside of the frequency content from wave excitation. This can be seen in **Fig. 4** where typical wave energy spectra are plotted. The second mode is typically at least $f_1=0.8$ Hz even for very large turbines and this is an area where wave energy is very low.
2. Low structural damping is assumed, typically a damping ratio of $\zeta_0=1.0\%$ (corresponding to a logarithmic decrement of $\delta_0=0.0628$) is used for offshore wind turbines founded on monopiles.
3. As structural damping is low, the response can be assumed to be narrow-banded and only the region close to the first natural frequency ω_0 is relevant for all terms which are a function of ω . Therefore, the following functions are replaced by a constant value (at $\omega = \omega_0$):
 - Wave number and wave length
 - Correction factor to take account of diffraction effects
 - Generalised wave loading (=hydrodynamic transfer function)
 - Wave energy spectrum
4. Drag loading is neglected as this is small for fatigue waves, see e.g. Kühn [4]. This assumption is valid for all typical monopile diameters ($D>4\text{m}$) for fatigue wave conditions encountered in the North or Baltic Sea. Also the effect of stretching wave kinematics to the wave crest is (inherently in the frequency domain method) neglected.
5. Hydrodynamic damping is neglected as the velocity of the structure is small.

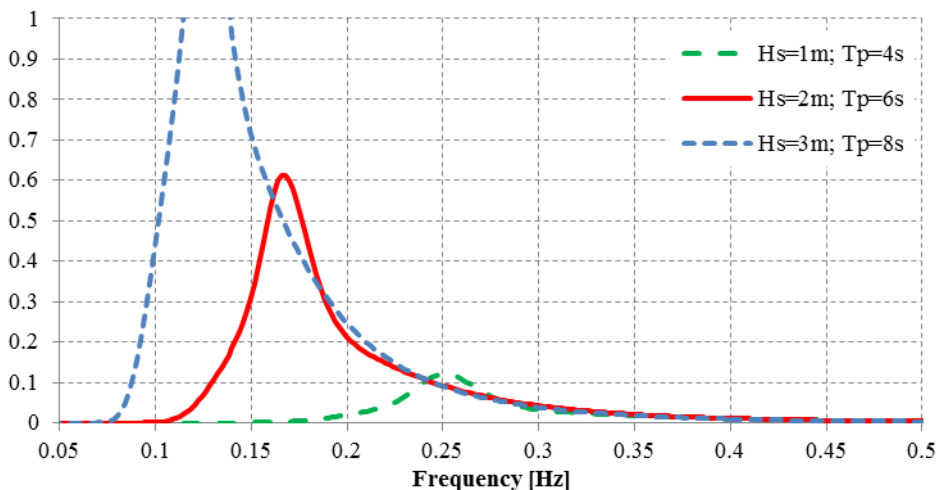


Fig. 4. Typical wave energy spectra (y-axis: Wave energy)

Abb. 4. Typische Wellenenergiespektren (y-Achse: Wellenenergie)

The individual steps and consequences of the simplifications made are further detailed in the following sections.

3.3 Mode shapes and generalized properties

Mode shapes $\Phi_n(z)$, eigenfrequencies ω_n and generalized properties (generalized mass M_n and generalized stiffness K_n for each mode) are determined based on mass and stiffness matrices for the full system. The properties for the first mode are denoted as $\Phi_0(z)$, ω_0 , M_0 and K_0 . The modal stiffness for the first mode shape with the amplitude at the centre of gravity (CoG) of the rotor-nacelle-assembly (RNA) normalized to “1” is denoted as $K_{0, \text{norm}}$.

3.4 Hydrodynamic transfer function

The hydrodynamic transfer function can be written as follows for each mode n :

$$H_{a,n}(\omega) = \hat{F}_{D,n}(\omega) + i \cdot \hat{F}_{M,n}(\omega)$$

$$= \underbrace{\omega \cdot \int_0^d c_n(z) \cdot \eta(z, \omega) \cdot \Phi_n(z) \cdot dz}_{\text{Drag term}} + i \cdot \underbrace{\rho \cdot \omega^2 \cdot \int_0^d C_M(z) \cdot \left[\pi \cdot \frac{D(z)^2}{4} \right] \cdot \eta(z, \omega) \cdot \Phi_n(z) \cdot dz}_{\text{Inertia term}}$$

with

- d: Water depth measured from seabed to still water level
- $c_n(z)$: Hydrodynamic damping coefficient
- $C_M(z)$: Inertia coefficient
- ρ : Density of sea water
- $D(z)$: Diameter of the structure at elevation z
- $\eta(z, \omega)$: Distribution function for wave kinematics, see below

Further details can be found in Hapel [2], chapter 4.4.

Wave number k and wave length λ are needed to determine the hydrodynamic transfer function. These quantities are functions of the wave frequency ω , with the value at the first natural frequency being determined from the dispersion equation:

$$\omega^2 = k \cdot g \cdot \tanh(k \cdot d) \rightarrow k(\omega_0) = k_0 \quad (3)$$

with

- g: Acceleration due to gravity

The wave length is determined based on the wave number as follows:

$$k = 2\pi / \lambda, \text{ i.e. } \lambda_0 = \frac{2\pi}{k_0} \quad (4)$$

Monopiles are big diameter structures, therefore diffraction needs to be taken into account. This is done by modifying the inertia coefficient, see van der Tempel [5]. Diffraction correction is performed for the wave length at first natural frequency, based on the following formula:

$$C_M(z) = -2.5 \cdot \left(\frac{D(z)}{\lambda_0} \right)^3 + 7.53 \cdot \left(\frac{D(z)}{\lambda_0} \right)^2 - 7.9 \cdot \left(\frac{D(z)}{\lambda_0} \right) + 3.2 \leq 2.0 \quad (5)$$

For monopiles, only the inertia term of Morison's equation is considered, i.e. drag contribution is neglected. The hydrodynamic transfer function is needed for the first mode shape only and this is written as follows:

$$H_{a,0} = \rho \cdot \omega_0^2 \cdot \int_0^d C_M(z) \cdot \left[\pi \cdot \frac{D(z)^2}{4} \right] \cdot \eta_0(z) \cdot \Phi_0(z) \cdot dz = \text{const} \quad (6)$$

The distribution function $\eta(z, \omega_0)$ is used to compute the wave kinematics over water depth d and is defined as follows for the wave frequency being equal to the first natural frequency:

$$\eta(z, \omega_0) = \eta_0(z) = \frac{\cosh(k_0 \cdot (z+d))}{\sinh(k_0 \cdot d)} \quad (7)$$

An example for this distribution function over water depth (below still water level) is shown in **Fig. 5** (left). It is obvious that the main wave loading originates from the zone close to the water line, where also the modal amplitude $\Phi_0(z)$ is largest. The integral as given in Eq. (6) is evaluated in the graph to the right of **Fig. 5** to emphasize this effect. It should be noted that this function becomes more steep when the natural frequency is higher, i.e. the relevant zone becomes more concentrated around the still water level.

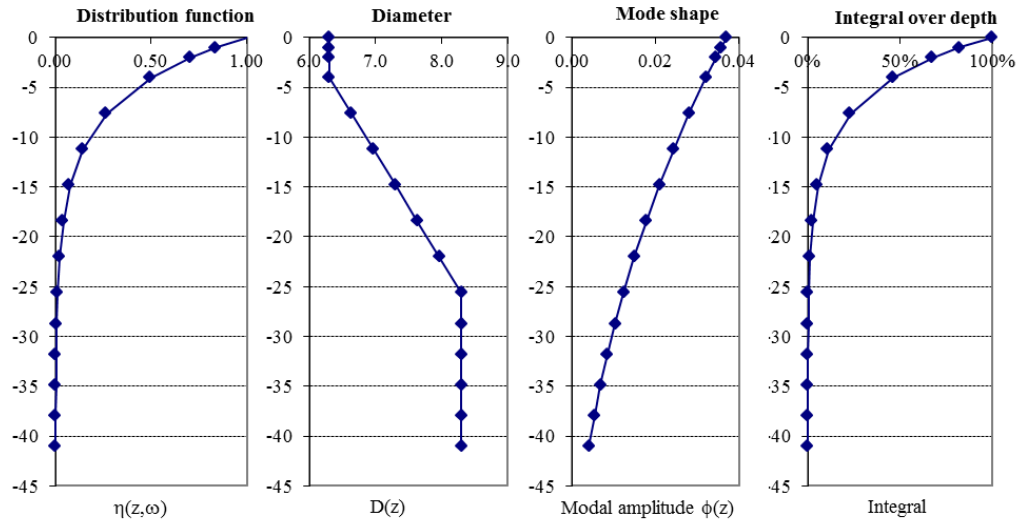


Fig. 5. Distribution function $\eta(z)$ for wave kinematics, structural diameter, modal amplitude and integral for hydrodynamic transfer function over water depth (0 = still water level, z negative towards seabed); still water level has been assumed to +1m LAT, therefore lowest elevation is z=-41m

Abb. 5. Verlaufsfunktion $\eta(z)$ für die Wellenkinematik, Strukturdurchmesser, Eigenformamplitude und Integral zur Ermittlung der hydrodynamischen Transferfunktion über Wassertiefe (0 = Ruhewasserspiegel, z ist negativ Richtung Seeboden); Ruhewasserspiegel wurde zu +1m LAT gesetzt, daher ist die größte Tiefe z=-41m

3.5 Mechanical transfer function

The mechanical transfer function for mode n is defined as:

$$H_n(\omega) = \frac{1}{1 - \left(\frac{\omega}{\omega_n}\right)^2 + 2 \cdot i \cdot \xi_n \cdot \frac{\omega}{\omega_n}} \cdot \frac{1}{K_n} \tag{8}$$

with ξ_n : Modal damping ratio for mode n

The absolute value of the transfer function for the first mode is received as:

$$|H_0(\omega)| = \frac{1}{\sqrt{\left[1 - \left(\frac{\omega}{\omega_0}\right)^2\right]^2 + 4 \cdot \xi_0^2 \cdot \left(\frac{\omega}{\omega_0}\right)^2}} \cdot \frac{1}{K_0} \tag{9}$$

3.6 Spectrum and variance of displacements

The quantities described before can now be used to determine the spectrum of displacements, see Eq. (2):

$$\begin{aligned} S_{uu}(z, \omega) &= |H(z, \omega)|^2 \cdot S_{\zeta\zeta}(\omega) \\ &= |\Phi_0(z) \cdot H_0(\omega) \cdot H_{a,0}(\omega)|^2 \cdot S_{\zeta\zeta}(\omega) \end{aligned} \tag{10}$$

The spectrum of displacements is calculated for each elevation z of relevance and for each frequency ω . If it is assumed that the hydrodynamic transfer function is constant for the relevant range close to the first natural frequency and when the hydrodynamic transfer function according to Eq. (6) is introduced, the following equation is obtained:

$$S_{uu}(z, \omega) = |\Phi_0(z) \cdot H_0(\omega)|^2 \cdot H_{a,0}^2 \cdot S_{\zeta\zeta}(\omega) \tag{11}$$

The variance of displacements for a specific sea state and the corresponding wave spectrum $S_{\zeta\zeta}(\omega)$ can be determined through integration of the response spectrum:

$$\begin{aligned}
\sigma_u^2(z) &= \int_{-\infty}^{+\infty} S_{uu}(z, \omega) d\omega \\
&= \int_{-\infty}^{+\infty} |\Phi_0(z) \cdot H_0(\omega)|^2 \cdot H_{a,0}^2 \cdot S_{\zeta\zeta}(\omega) \cdot d\omega \\
&= \Phi_0(z)^2 \cdot H_{a,0}^2 \cdot \int_{-\infty}^{+\infty} |H_0(\omega)|^2 \cdot S_{\zeta\zeta}(\omega) \cdot d\omega
\end{aligned} \tag{12}$$

Assuming that the wave energy spectrum is constant for the relevant range close to the first natural frequency, i.e. $S_{\zeta\zeta}(\omega)$ is replaced by $S_{\zeta\zeta}(\omega) = S_{\zeta\zeta}(\omega_0) = \text{const.}$, the following is obtained:

$$\sigma_u^2(z) = \Phi_0(z)^2 \cdot H_{a,0}^2 \cdot S_{\zeta\zeta}(\omega_0) \cdot \int_{-\infty}^{+\infty} |H_0(\omega)|^2 \cdot d\omega \tag{13}$$

The integral $\int_{-\infty}^{+\infty} |H_0(\omega)|^2 \cdot d\omega$ (see Eq. (9)) can be solved analytically and the solution is:

$$\int_{-\infty}^{+\infty} |H_0(\omega)|^2 \cdot d\omega = \frac{1}{K_0^2} \cdot \frac{\pi}{4 \cdot \xi_1} \cdot \omega_0 \tag{14}$$

The following formula for the variance of displacements is then received:

$$\sigma_u^2(z) = \Phi_0(z)^2 \cdot H_{a,0}^2 \cdot S_{\zeta\zeta}(\omega_0) \cdot \frac{1}{K_0^2} \cdot \frac{\pi}{4 \cdot \xi_0} \cdot \omega_0 \tag{15}$$

From this, the standard deviation (RMS) of displacements at the center of gravity (CoG) of nacelle mass (z_{nac}) can be determined.

$$\sigma_{u,nac} = \sqrt{\sigma_u(z = z_{nac}, \omega_0)^2} = \sqrt{\Phi_0(z)^2 \cdot H_{a,0}^2 \cdot S_{\zeta\zeta}(\omega_0) \cdot \frac{1}{K_0^2} \cdot \frac{\pi}{4 \cdot \xi_0} \cdot \omega_0} \tag{16}$$

3.7 Standard deviation of bending moments

From the RMS of displacements at tower top the RMS of tower bottom bending moments can be calculated by applying the following equation:

$$\begin{aligned}
\sigma_{M,TB} &= \sigma_{u,nac} \cdot \omega_0^2 \cdot \int_{z=z_{TB}=0}^{z=z_{nac}} \Phi_0(z) \cdot \mu(z) \cdot z \cdot dz \\
&= \sigma_{u,nac} \cdot H_{TB}
\end{aligned} \tag{17}$$

with z_{TB} : Elevation at tower bottom (interface to monopile)
 z_{nac} : Elevation at CoG of RNA (relative to elevation at tower bottom)
 $\mu(z)$: Mass per length

This equation simply assumes that the bending moment at tower base can be calculated by integration of inertia forces along the structure. The biggest contribution originates from the mass of the RNA.

3.8 Damage equivalent loads (DELs)

As the last step, damage equivalent loads (DELs) are determined from the variance based on narrow band assumptions as follows:

$$\Delta M_{eq} = DEL = (8 \cdot m_0)^{0.5} \cdot \left[\Gamma \left(\frac{2+m}{2} \right) \right]^{(1/m)} \quad (18)$$

with m_0 : zeroth spectral moment of quantity used
 Γ : gamma function

This formula has been taken from Barltrop [3], Fig. 11.12, page 616, where this is called “effective constant amplitude stress” (here moments are considered, but the principle is identical).

In this formula, m is the inverse slope of the S-N-curve. For steel, the S-N-curve does have inverse slopes of $m=3$ and $m=5$. As a typical value $m=4$ can be used, hence:

$$\text{With } \left[\Gamma \left(\frac{2+4}{2} \right) \right]^{(1/4)} = 1.189$$

$$\Delta M_{eq} = (8 \cdot m_0)^{0.5} \cdot 1.189 = 3.363 \cdot \sqrt{m_0} \quad (19)$$

$(m_0)^{0.5}$ is the standard deviation of the bending moment (e.g. at tower bottom), hence:

$$\Delta M_{eq} = (8 \cdot m_0)^{0.5} \cdot 1.189 = 3.363 \cdot \sigma_{M,TB} \quad (20)$$

This is the damage equivalent moment ΔM_{eq} for the number of cycles given as:

$$N_{ref} = f_0 \cdot T \quad (21)$$

with T : Time in seconds

The number of cycles is thus dependent on the natural frequency f_0 of the specific structure, which is inconvenient. Usually, so-called “1-Hz-DELs” are used, where the number of reference cycles is defined as the number of seconds within the interval T , i.e:

$$N_{ref1Hz} = T \quad (22)$$

The damage equivalent moment (19) does need to be converted to take account of the different number of cycles. Finally, the DEL can be converted considering the (constant) inverse slope of the S-N-curve as follows, assuming $m=4$ for steel:

$$\Delta M_{eq,Nref1Hz} = 3.363 \cdot \sigma_{M,TB} \cdot \left(\frac{N_{ref}}{N_{ref1Hz}} \right)^{(1/m)} = 3.363 \cdot \sigma_{M,TB} \cdot (f_0)^{0.25} \quad (23)$$

$\Delta M_{eq,Nref1Hz}$ is independent of the intended service life. The 1-Hz-DEL is combined with the number of seconds during intended service life to arrive at the total damage.

4 Summarized formula

All the steps executed so far can now be summarized into one formula as follows:

$$\begin{aligned}
 \Delta M_{eq,Nref1Hz} &= 3.363 \cdot \sigma_{M,TB} \cdot (f_0)^{0.25} \\
 &= 3.363 \cdot \sigma_{u,nac} \cdot H_{TB} \cdot (f_0)^{0.25} \\
 &= 3.363 \cdot \sqrt{\left(\Phi_0(z_{nac})^2 \cdot H_{a,0}^2 \cdot S_{\zeta\zeta}(\omega_0) \cdot \frac{1}{K_0^2} \cdot \frac{\pi}{4 \cdot \xi_0} \cdot \omega_0 \right)} \cdot H_{TB} \cdot (f_0)^{0.25} \quad (24) \\
 &= 3.363 \cdot \Phi_0(z_{nac}) \cdot H_{a,0} \cdot \sqrt{S_{\zeta\zeta}(\omega_0)} \cdot \frac{1}{K_0} \cdot \sqrt{\frac{1}{\xi_0}} \cdot \sqrt{\frac{\pi}{4}} \cdot \sqrt{\omega_0} \cdot H_{TB} \cdot \left(\frac{\omega_0}{2\pi} \right)^{0.25} \\
 &= 1.8825 \cdot \Phi_0(z_{nac}) \cdot H_{a,0} \cdot \sqrt{S_{\zeta\zeta}(\omega_0)} \cdot \frac{1}{K_0} \cdot \sqrt{\frac{1}{\xi_0}} \cdot \omega_0^{3/4} \cdot H_{TB}
 \end{aligned}$$

The final expression to determine DELs for a specific sea state becomes:

$$\Delta M_{eq,Nref1Hz} = 1.8825 \cdot \sqrt{S_{\zeta\zeta}(\omega_0)} \cdot \frac{\Phi_0(z_{nac})}{K_0} \cdot \sqrt{\frac{1}{\xi_0}} \cdot \omega_0^{3/4} \cdot H_{a,0} \cdot H_{TB} \quad (25)$$

With:

$$H_{TB} = \omega_0^2 \cdot \int_{z=z_{TB}=0}^{z=z_{nac}} \Phi_0(z) \cdot \mu(z) \cdot z \cdot dz \quad \text{Transfer function to tower bottom} \quad (26)$$

$$H_{a,0} = \rho \cdot \omega_0^2 \cdot \int_0^d C_M(z) \cdot \left[\pi \cdot \frac{D(z)^2}{4} \right] \cdot \eta_0(z) \cdot \Phi_0(z) \cdot dz \quad \text{Hydrodynamic transfer function} \quad (27)$$

These formulas can be easily evaluated analytically, only modal analysis needs to be performed numerically.

This expression has proven to give excellent results for tower bottom, as the assumption of a narrow band response is valid at this elevation. At seabed, deviations to results from full frequency domain or time domain calculations may be larger, depending on whether the resonant part of the response is governing or whether quasi-static response is of higher importance. Typically, fatigue loads are still within 10% accuracy at seabed as well.

Some important conclusions can be drawn from this expression:

1. DELs are proportional to $(1/\xi_0)^{0.5}$ – i.e. if damping is e.g. doubled, then fatigue loads decrease by 30% !
2. Damage is proportional to the square root of spectral wave energy at the first natural frequency. This is important when lumping of the scatter diagram shall be performed.
3. Mode shape and hydrodynamic properties around the still water level are of particular importance. The hydrodynamic transfer function is linearly proportional to mode shape amplitudes in the wave loaded zone, as can be seen from Eq. (27). Reducing modal amplitude below still water level is therefore particularly helpful to reduce fatigue loads.
4. In total, fatigue loads are proportional to ω_0^3 , when all other parameters are unchanged. This is an indication that a large head mass (from the turbine) is not necessarily disadvantageous, as this decreases the natural frequency.

5 Validation

This method has been used in many projects, with excellent results for nearly all cases. One example is shown in **Fig. 6**. Here, results for pure wave loading determined with the proposed method are compared with results determined by simulation in the time domain and subsequent rainflow counting. Considerable scatter can be seen, as can be expected for a stochastic process, particularly because only 10 minute periods are simulated in the time domain. On average, the simplified method does almost perfectly match the simulations in the time domain.

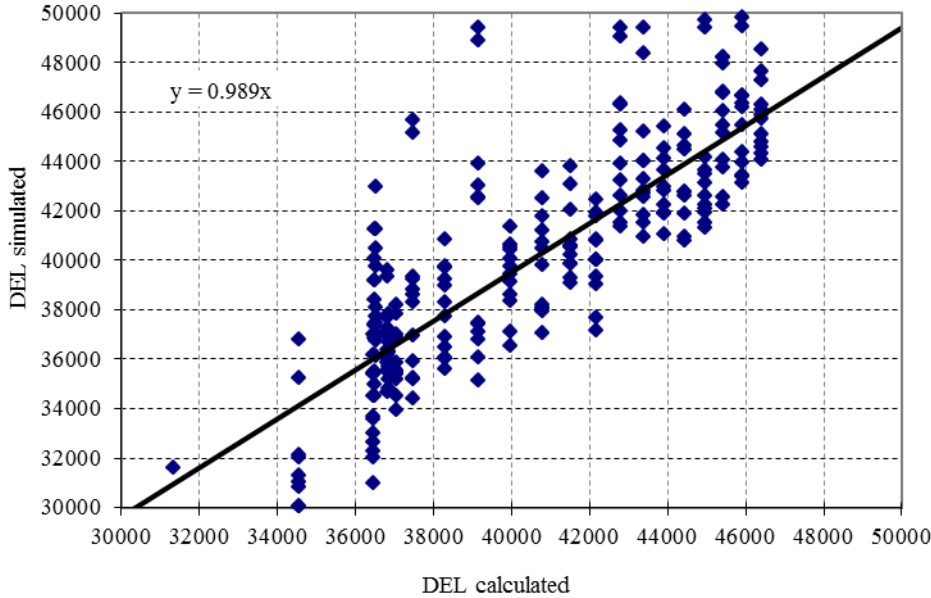


Fig. 6. Comparison of DELs determined by the simplified method (DEL calculated) vs. DEL simulated in the time domain

Abb. 6. Vergleich von schadensäquivalenten Einstufenkollektiven (DEL) für die vorgeschlagene Methode im Vergleich mit Ergebnissen aus der Simulation von Zeitreihen

6 Conclusions

6.1 Lumping of the scatter diagram

As fatigue loads are depending on the wave energy at first natural frequency, lumping of the scatter diagram must be performed based on the spectral value at first natural frequency and an equivalent spectral energy can be determined for the entire scatter diagram as follows:

$$\sqrt{S_{\zeta\zeta}(\omega_0)_{eq}} = \left(\frac{\sum_n \left[\sqrt{S_{\zeta\zeta}(H_{S,n} | T_{P,n} | \omega_0)} \right]^m \cdot p(n)}{\sum_n p(n)} \right)^{1/m} \quad (28)$$

with $p(n)$: Probability for sea state n with $H_{S,n}$ and $T_{P,n}$

This equation is based on the following considerations:

- a) DEL are proportional to $\sqrt{S_{\zeta\zeta}(\omega_0)}$, see Eq. (25)
- b) Damage incurred by each sea state is proportional to $(DEL)^m$

It follows from a) and b) that weighting must be performed based on $\left(\sqrt{S_{\zeta\zeta}(\omega_0)}\right)^m$ for each sea state, which directly leads to Eq. (28).

Weighting can be performed in two stages:

- 1) An equivalent H_S is found based on quasi-static considerations.
- 2) An equivalent T_P is found based on equivalent spectral energy.

This ensures that both quasi-static and resonant contributions of the response are adequately covered.

6.2 Site parameter

If Eq. (25) is simplified, it can be stated that fatigue loads are proportional to the following parameter S :

$$S = \frac{\omega_0^{0.75}}{K_{0,norm}} \cdot \sqrt{S_{\zeta\zeta}(\omega_0)_{eq}} \cdot \sqrt{\frac{1}{\xi}} \cdot H_{TB} \cdot H_{a,0} \quad (29)$$

This site parameter can be used to evaluate fatigue loads for all positions within a wind farm. Load simulation can be performed for the sites having minimum and maximum site parameter and interpolation can be used in between. This has been used successfully within the certification of an offshore wind farm.

7 Summary

In this paper, expressions to determine wave induced fatigue damage have been derived based on frequency domain considerations. Simplifications relevant for monopile substructures have been used to determine a compact formula which allows rapid calculation of wave induced fatigue loads. This expression can further be used to derive expressions for a “Site parameter” for interpolation of fatigue loads and an expression for the equivalent spectral energy, which can be used for lumping of a scatter diagram.

References

- [1] *Seidel, M.*: 6MW Turbines with 150m+ Rotor Diameter - What is the Impact on Substructures? Conference proceedings DEWEK: Bremen 2012.
- [2] *Hapel, K.-H.*: Festigkeitsanalyse dynamisch beanspruchter Offshore-Konstruktionen. Braunschweig: Vieweg, 1990.
- [3] *Barltrop, N.; Adams, A.*: Dynamics of fixed marine structures. Oxford: Butterworth-Heinemann 1991.
- [4] *Kühn, M.*: Dynamics and Design Optimisation of Offshore Wind Energy Conversion Systems. Ph.D. thesis, Delft 2001.
- [5] *Van der Tempel, J.*: Design of Support Structures for Offshore Wind Turbines. Ph.D. thesis, Delft 2006.

Author:

Dr.-Ing. Marc Seidel

Senvion SE

Franz-Lenz-Straße 1

49084 Osnabrück

Email: marc.seidel@senvion.com